ISSN 1648-7788 / eISSN 1822-4180

VILNIUS TECH
Vilnius Gediminas Technical University

AVIATION

2025
Volume 29
Issue 1
Pages 1–10
https://doi.org/10.3846/aviation.2025.23154

COMPARATIVE EFFICIENCY TESTING OF A COMPOSITE HYDRAULIC CYLINDER

Michał STOSIAK [1]✉, Marek LUBECKI [2], Michał BANAŚ [3]

[1, 3]*Faculty of Mechanical Engineering, Wrocław University of Science and Technology, Wrocław, Poland*
[2]*Komes Group Ltd., Wrocław, Poland*

Article History:
- received 31 December 2024
- accepted 16 January 2025

Abstract. The paper points to the increasing use of composite materials in hydraulic components. This entails many benefits, such as weight reduction which is particularly important in aviation. However, new problems arise with the use of new materials. With regard to a hydraulic actuator whose cylinder is made of a composite material, one of the issues is ensuring adequate efficiency, comparable to that of a steel cylinder. The efficiency of a hydraulic actuator is related to friction processes in the structural nodes and to leaks in the cylinder. This paper presents the original results of volumetric, hydraulic-mechanical and total efficiency tests of three designs differing in the material used as a liner of a cylinder. The materials considered as liner were CFRP composite, polyurethane F180. In addition, a steel liner was considered as a reference. Variations in actuator efficiency depending on the liner used were indicated.

Keywords: lightweight hydraulic, cylinder, composite materials, efficiency, aviation, aircraft hydraulic drives.

✉Corresponding author. E-mail: *michal.stosiak@pwr.edu.pl*

1. Introduction

In mechanical, transport and aerospace engineering's, one of the most common types of drive is the hydrostatic drive. It consists of a pump that converts kinetic energy (usually the rotational movement of a shaft) into energy of fluid pressure, a set of valves whose task is to control flow parameters (flow rate, direction, pressure), receivers (motors and actuators) that convert the energy of fluid pressure into mechanical energy, and other elements such as pipes or accumulators. The popularity of this type of system is due to a number of advantages, such as the high power-to-weight ratio, the possibility of free arrangement of components on the machine or the possibility of obtaining almost any functional structure, as well as the ease of automation (Vacca, 2021; Stosiak & Karpenko, 2024). Hydraulic systems often perform critical functions. They are commonly found in heavy-duty machinery, mobile machinery, agricultural and forestry machinery, floating vessels, aircraft and many others (Karpenko, 2022; Kilikevicius et al., 2019). In many applications it is very important to reduce the weight of equipment, systems and their components. This is particularly important in mobile machinery and aviation. In aviation, the reduction of the weight of the equipment components of a flying object makes it possible to transport heavier loads with the same propulsion power or to reduce the propulsion power with the same weight of the transported load. Weight reduction in flying objects contributes to reduced fuel consumption and increased flight range. Weight reduction in hydraulic components is achieved by reducing dimensions (microhydraulics) or by using new materials. Composite materials are of interest to designers of modern lightweight hydraulic systems due to their many advantages.

Interest in the use of fibre-reinforced composite materials is growing year on year. This is due to their high strength, low weight and corrosion resistance (Wypych, 2016; Kaw, 2005; Karpenko et al., 2023; Karpenko & Nugaras, 2022; Sanchez-Sobrado et al., 2024). New materials, including composite materials, are increasingly being used in the design of hydraulic components, according to Lubecki et al. (2022). A composite is a material obtained by combining two or more base materials with radically different properties (Bogdevičius et al., 2021). The resulting material has superior and/or novel properties compared to components used separately or resulting from their summation, according to Wypych (2016). In most cases, one of the materials plays the role of the matrix (continuous, bonding medium), while the rest becomes the filler (reinforcement). Among fibre composites (in which reinforcement is realised by fibres), one can distinguish two main types: those reinforced with chopped (short) fibres and those reinforced with continuous fibres (Datoo, 1991). Fibres (usually glass, carbon or aramid) are characterised by a high modulus of elasticity along their axis and high tensile strength. When stored and processed

correctly, they do not show a decrease in properties during the technological process, and differences in diameter and properties between individual fibres of the same type are negligibly small. Continuous fibres are mostly made by pyrolytic carbonisation of polyacrylonitrile (PAN) fibres (Wypych, 2016). Depending on the precursor used and the parameters of the technological process, the density of the finished fibres is in the range of 1.6–2.0 g/cm^3, with the density of most precursors being between 1.14 and 1.19 g/cm^3 (Chawla, 2012). Many types of such fibres can be found on the market, differing in their parameters and therefore also in their price. Figure 1 and Figure 2 show charts made available by leading carbon fibre manufacturers presenting their portfolio. These show that fibres are divided into three main groups according to their Young's modulus, with medium modulus fibres achieving the highest strengths (even over 6000 MPa). The strength range of carbon fibres extends from about 2800 MPa to the already mentioned over 6000 MPa, while the modulus ranges from about 220 GPa to over 500 GPa (Teijin Carbon Fiber Business, 2024; Toray Composite Material America Inc., 2021).

The second component of the composite material is the matrix, the purpose of which is to bind the reinforcement material together and to allow load transfer between fibres. It can also stop or slow the propagation of cracks initiated in the reinforcement and protect the fibres from adverse environmental conditions. The most commonly used matrix materials include polyester, vinyl ester, epoxy resins and thermoplastics (PE, PP, PA) (Wypych, 2016; Chawla, 2012; Gibson, 2016). There are many ways to manufacture fibre-reinforced polymer composite materials, such as lamination (hand, spray, vacuum bag), infusion moulding, winding, weaving or pultrusion, according to Wypych (2016). In the manufacture of high-pressure cylinders and tanks, winding and weaving methods have mainly been used (Błażejewski et al., 2024).

The paper Solazzi (2019), shows the design process of a composite hydraulic cylinder. The author presents strength calculations for the cylinder taking into account its heterogeneity (presence of an internal aluminium liner and

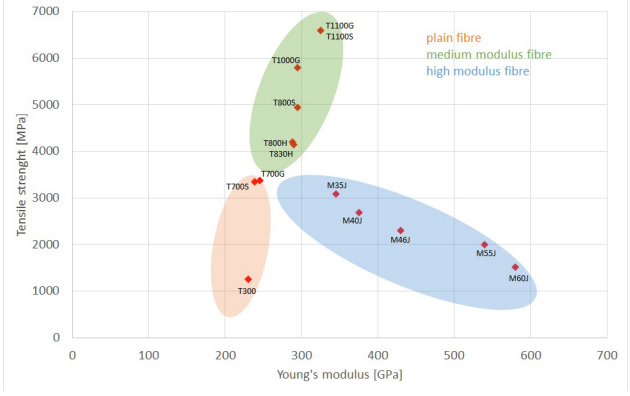

Figure 1. Diagram showing the Young's modulus and strengths of the different types of Torayca carbon fibre offered by TORAY (source: Authors elaboration based on Toray Composite Material America Inc., 2021)

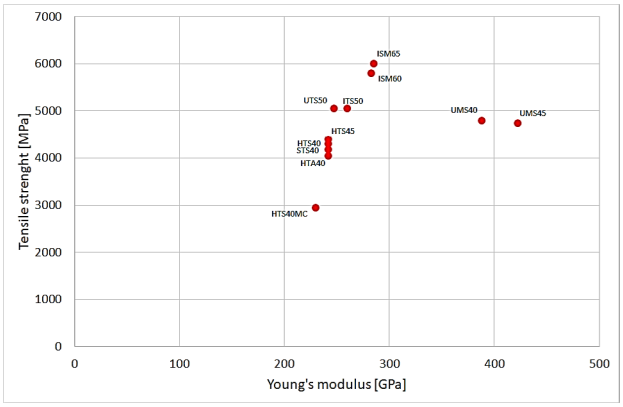

Figure 2. Diagram showing the Young's modulus and strengths of the different types of TENAX carbon fibre offered by Taijin (source: Authors elaboration based on Teijin Carbon Fiber Business, 2024)

an external composite reinforcement). The Huber-Mises hypothesis was used to assess the strength. The bottom, gland and liner were made of aluminium alloy and then joined together by welding. A composite reinforcement made of carbon fabric was then made on the prepared component using the vacuum bag lamination method. In addition, the composite piston rod is presented, along with the method of connecting the aluminium piston and ear to the composite piston rod using a shaped connection. In the last part of the paper, experimental tests of the finished actuator on a test stand are presented. Ulbricht et al. (2016) presented potential applications of composite materials in hydrostatic drive components in light of the Industry 4.0 concept. One of the applications presented was a bladder accumulator made of carbon fibre-reinforced composite. The authors outlined the design, fabrication and testing process of such an element showing several similarities to Generation IV high-pressure tanks. The paper also demonstrates the possibilities of monitoring such structures by embedding displacement, strain, temperature or other sensors during fabrication. Scholz and Kroll (2014) considered removing the steel liner from the inside of the cylinder and replacing it with a nanocomposite coating with properties that provide suitable tribological conditions at the cylinder-piston interface.

There are papers addressing the design of hydraulic actuators using composite materials, while signalling a number of design problems. One problem is ensuring adequate frictional interaction between the piston seal and the inner surface of the cylinder. In most cases, this is solved by using a thin-walled tube made of steel or aluminium alloy (so-called liner), which is reinforced with a composite overwrap (Mantovani, 2020; Nowak & Schmidt, 2013; Nowak & Schmidt, 2014; Solazzi, 2019, 2021; Wang et al., 2018; Stelling et al., 2014; Szczepaniak & Jastrzębski, 2020). Despite its widespread use, this solution also has disadvantages. The difference in stiffness as well as in the temperature expansion coefficients of the two materials can lead to stresses and cracks, especially under prolonged fatigue loads (Gibson, 2016; Nowak & Schmidt,

2015; Rozumek & Macha, 2009; Rozumek et al., 2017; Liu & Shi, 2019; Rozumek & Bański, 2012). Another approach is to use a polymer or nanocomposite liner (Scholz & Kroll, 2014), which, however, entails the additional complexity of manufacturing technology associated with the application of such a layer. The simplest solution is to get rid of the liner and leave the inner composite surface of the cylinder (El Assward et al., 2018; Elassward et al., 2018). However, such solution can increase the frictional force and may not provide adequate cylinder sealing, thus leading to a decrease in efficiency.

This paper examines the effect of different types of liner, or lack thereof, on the efficiency of a composite double-acting hydraulic actuator with a single-sided piston rod. Three types of cylinders – without liner, with steel liner and with polymer liner – were considered and tested in the study. The polymer liner material was selected through a series of tests to determine the adhesion to the cylinder material and tribological properties (friction coefficient, wear).

Section 2 presents the materials chosen for the liner tests and gives the parameters of the actuator under test. Section 3 presents the test rig with the test tracks and gives the mathematical equations used to determine the actuator efficiency. Section 4 presents the results obtained for the volumetric, hydraulic-mechanical and total efficiency of the test actuators for the extension and retraction movement phases. Furthermore, Section 4 compares the total efficiency of the actuators for different liner materials. Section 5 is the conclusions and observations.

2. Composite cylinder for hydraulic actuator

The selected types of cylinders were manufactured using filament winding method, and their deformations during tie-rods preloading and internal pressure loading were measured. The strain measurements allowed for verification of the correctness of the strength calculations of the cylinders (Lubecki et al., 2023). In order to finally accept or reject specific types of internal surfaces, the efficiencies of the complete actuators were also determined. A comparison was also made between the composite cylinder and a conventional steel cylinder. The composite cylinder was part of an actuator that was held together using tie-rods. This was dictated by the simplicity of the design. It is not advisable to drill or thread the composite parts due to the drastic reduction in mechanical properties of the joint so obtained. The initial design parameters are summarised in Table 1.

Table 1. Initial design parameters of the actuator

Parameter	Value
Operating pressure [MPa]	15
Max piston speed [m/s]	0.3
Operating stroke [mm]	150
Cylinder inner diameter [mm]	40

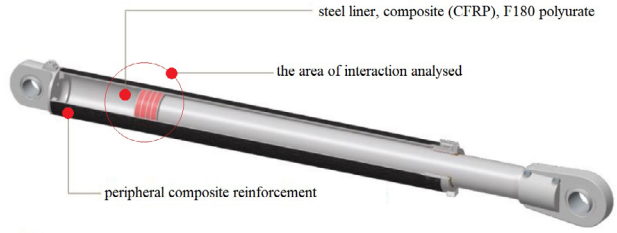

Figure 3. An overview of the composite cylinder liner and piston seal interaction area (source: based on the Parker Hannifin Corporation, 2017)

A total of 3 cylinders differing in internal surface material were tested. Figure 3 gives an illustrative view of the cylinder liner and piston seal interaction area.

Table 2 shows the weights of the individual cylinders and compares them with a reference steel cylinder with a wall thickness of 5 mm, made from commercially available stock. As can be seen, the weight reduction with composite reinforcement is very high, ranging from 67.6% for cylinder with steel liner to more than 91% for the one with polymer (polyurethane F180) liner.

Table 2. Comparison of masses of fabricated cylinders

Cylinder	Weight [g]	Difference, %
Steel	1704	–
composite without liner (CFRP)	136.7	91.9
composite, polymer liner (F180)	149.6	91.2
composite, steel liner	552.0	67.6

3. Bench testing of a composite hydraulic cylinder

Figure 4 shows a hydraulic diagram of the designed and built actuator test stand. The test stand enables cyclic extension and retraction of the tested actuator at pre-set speeds and under a pre-set load. The direction of movement of the actuator is changed by a directional control valve (4), while the velocity of movement can be set independently for both directions using flow regulators (5) and (6). The load is provided by a load actuator (15) connected to the pressure control valve (18), which enables the load pressure to be maintained independently of the flow rate (actuator velocity). The system allows pressures in the test actuator chambers, flow rates, piston rod position and load force to be recorded. Table 3 shows the data of the control and measuring instruments with which the bench was equipped.

The total efficiency of the actuator η_c was determined using the formula (Szydelski, 1999):

$$\eta_c = \frac{W_{out}}{W_{in}}, \tag{1}$$

where, W_{out} – the output energy obtained during movement of the actuator [J]; W_{in} – the input energy supplied to the actuator [J].

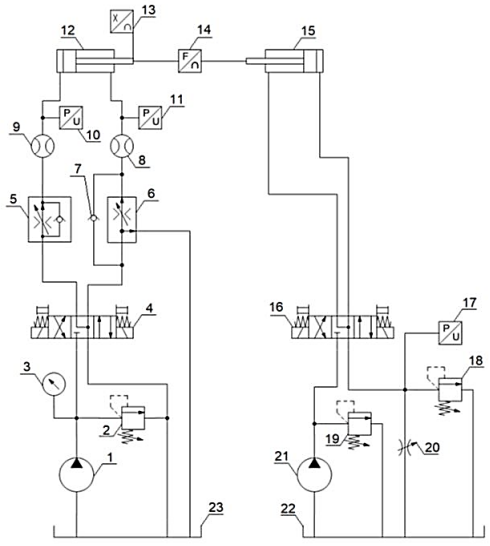

Figure 4. Hydraulic diagram of the actuator test rig: 1 – pump, 2 – safety valve, 3 – pressure gauge, 4 – 4/3 directional control valve, 5 – 2-way flow regulator, 6 – 3-way flow regulator, 7 – check valve, 8, 9 – flow meter, 10, 11 – pressure sensor, 12 – tested actuator, 13 – position sensor, 14 – force sensor, 15 – load actuator, 16 – 4/3 directional control valve, 17 – pressure sensor, 18 – pressure control valve, 19 – safety valve, 20 – adjustable throttle valve, 21– pump, 22, 23 – tank

The energy delivered to the actuator was determined as (Szydelski, 1999):

$$W_{in} = \int_0^T p(t) \cdot Q(t)\, dt, \tag{2}$$

where: T – stroke time [s]; $p(t)$ – pressure as a function of time [Pa]; $Q(t)$ – flow rate as a function of time [m^3/s].

The energy gained during the movement of the actuator was determined using the formula (Szydelski, 1999):

$$W_{out} = \int_0^T F(t) \cdot v(t)\, dt, \tag{3}$$

where: $F(t)$ – axial force acting on the piston rod [N]; $v(t)$ – piston velocity [m/s].

The volumetric efficiency η_v was determined using the formula (Szydelski, 1999):

$$\eta_v = \frac{V_t}{V_r}, \tag{4}$$

where: V_t – theoretical volume of the actuator chamber [m^3]; V_r – actual volume of fluid supplied to the actuator chamber [m^3].

The theoretical volume of the actuator chamber can be determined from the relationship that describes the piston chamber and the piston rod chamber:

$$V_t = \begin{cases} \pi \dfrac{D_w^2}{4} \cdot s \text{ for the piston chamber} \\ \pi \dfrac{D_w^2 - D_r^2}{4} \cdot s \text{ for the piston rod chamber} \end{cases}, \tag{5}$$

where: D_w – inside diameter of cylinder [m]; D_r – diameter of the piston rod [m]; s – stroke length [m].

The actual volume of fluid supplied to the actuator chamber can be determined from the relationship:

$$V_r = \int_0^T Q(t)\, dt. \tag{6}$$

The total efficiency of an actuator, when looking at the loss structure, can be expressed as the product of the volumetric efficiency and the hydraulic-mechanical efficiency:

$$\eta_c = \eta_v \cdot \eta_{hm}. \tag{7}$$

The hydraulic-mechanical efficiency η_{hm} was determined as:

$$\eta_{hm} = \frac{\eta_c}{\eta_v}. \tag{8}$$

4. Test results

4.1. The efficiency of an actuator with a steel cylinder

Figures 5a and 5b show examples of piston chamber pressures and axial force acting on a piston rod as a function of time during piston rod extension. These values

Table 3. Technical parameters of the test bench instrumentation

No. on the diagram	Device	Measured parameter	Unit	Measuring range	Class	Type / designation / serial number	Manufacturer
8	Flowmeter	Q_{tk}	dm^3/min	0.16–16	0.3	VC 0.2 F1 PS	KRACHT
9	Flowmeter	Q_{tc}	dm^3/min	0.4–80	0.3	VC 1 F1 PS	KRACHT
10, 11	Pressure sensor	p_{tk}, p_{tc}	MPa	25	0.6	PT-5101	SPAIS
13	Position sensor	x	mm	±150	0.5	PTx300	Peltron
14	Force sensor	F	kN	0–30	0.1	DiR3-3.0 Nr80275	ZDKP-PIMR
17	Pressure sensor	p_1	MPa	0–10	1	A-10 10MPa	WIKA
–	Acquisition card	–	–	–	0.1	Spider8	Hottinger Baldwin Messtechnik
–	Signal amplifier	–	–	–	0.6	AT-5230	SPAIS

where: Q_{tk} – flow rate to the piston chamber; Q_{tc} – flow rate to the piston rod chamber; p_{tk} – pressure at the piston chamber; p_{tc} – pressure at the piston rod chamber; p_l – pressure of external load.

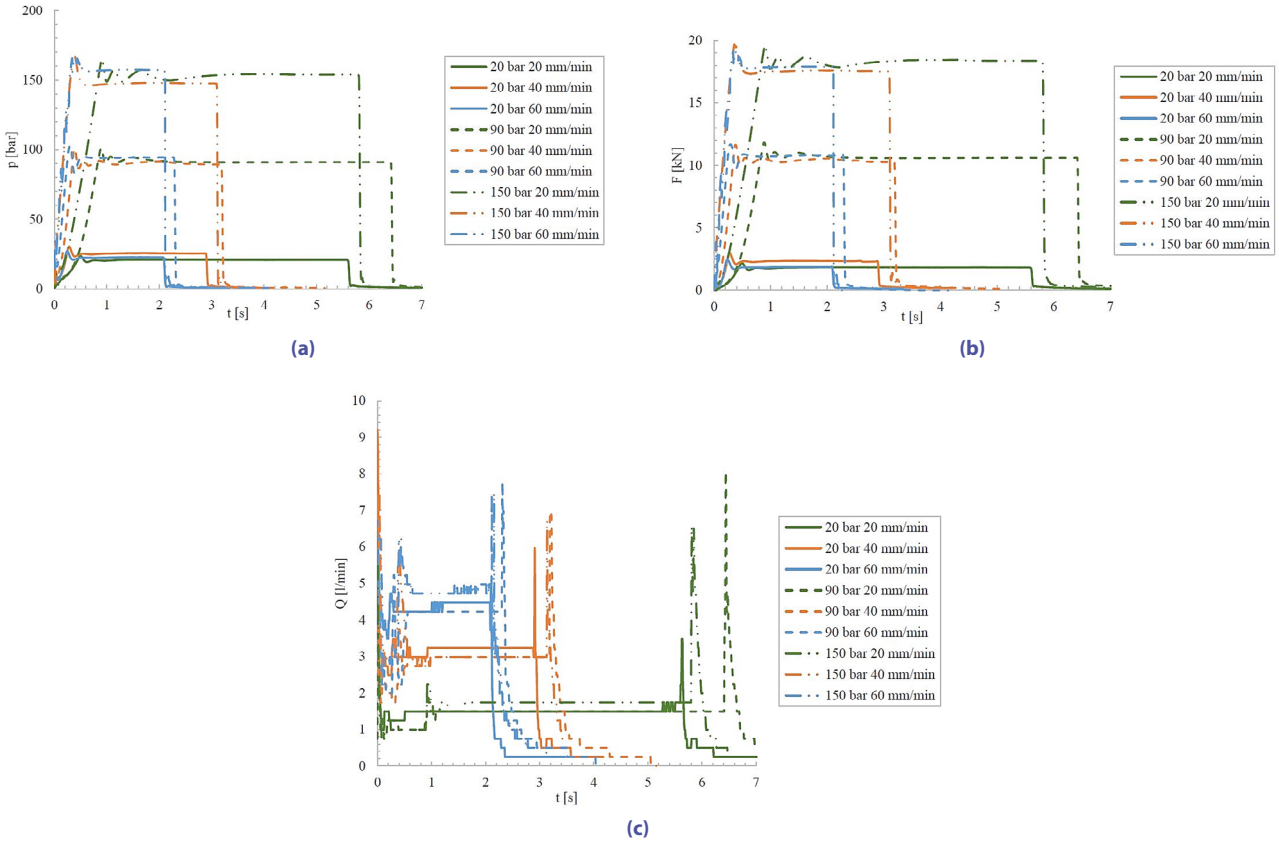

Figure 5. Exemplary test results for one stroke: (a) – pressure in the piston chamber of the actuator as a function of time during extension; (b) – force acting on a piston rod as a function of time during extension; (c) – fluid flow rate in the piston chamber as a function of time during extension

were recorded for steady-state pressures of 2 MPa, 9 MPa and 15 MPa and piston rod velocities of 20 mm/min, 40 mm/min and 60 mm/min. Figure 4c shows the flow rate of the fluid flowing into the piston chamber as a function of time during piston rod extension. It allowed for the amount of energy supplied and gained to be determined and the efficiency to be calculated. The values obtained for the steel cylinder actuator were used as a reference to evaluate composite designs. Similar tests were performed for composite cylinder actuators with and without liner.

Figure 6a shows the total efficiency of the actuator during piston rod retraction. The lowest efficiency (68%) was obtained for a pressure of 2 MPa and a velocity of 60 mm/s, while the highest efficiency (99%) was obtained for a pressure of 9 MPa and a velocity of 20 mm/s. At pressures of 9 MPa and 15 MPa, efficiencies exceeded 90% for all velocities. Figure 6b shows the total efficiency of the actuator during piston rod extension. As for the retraction, the lowest efficiency (65%) was recorded for a pressure of 2 MPa and a velocity of 20 mm/s, while the highest efficiency (93%) was recorded for a pressure of 15 MPa and a velocity of 60 mm/s. Again, for pressures of 9 MPa and 15 MPa, all efficiencies were above 90%.

In Figure 6, it can be seen that as the pressure inside the cylinder increases, the total efficiency increases.

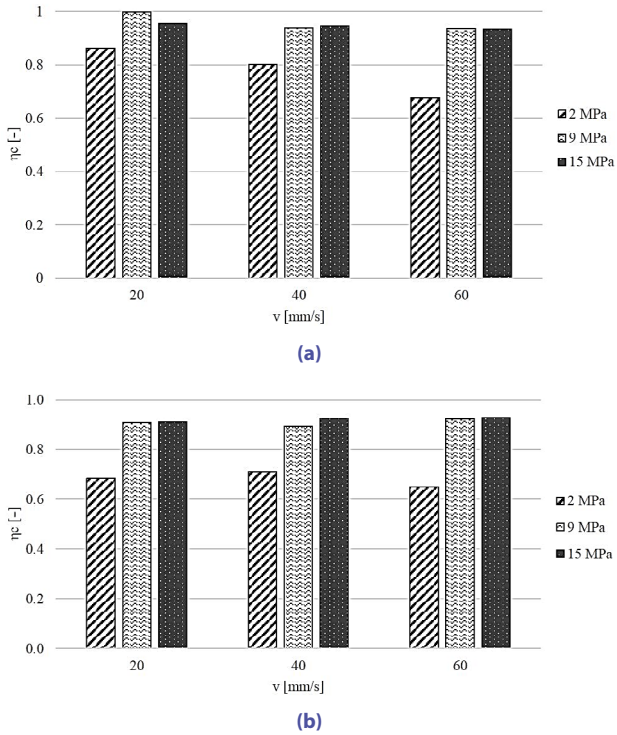

Figure 6. Overall efficiency of a steel cylinder actuator during: (a) – retraction; (b) – extension

Figure 6a and Figure 6b show the volumetric efficiencies η_v of an actuator with a steel cylinder during piston rod retraction and extension, respectively. For retraction, these efficiencies vary between 95% and 100% and in most cases, it can be seen that an increase in pressure causes a slight decrease in η_v. For extension, on the other hand, η_v varies between 89% and 99%, with the highest values recorded at 2 MPa.

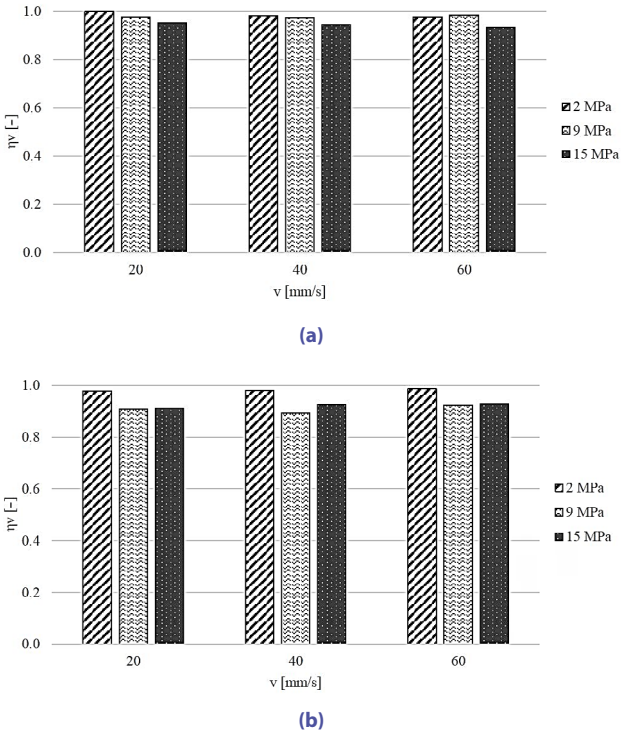

Figure 7. Volumetric efficiency of actuator with steel cylinder during: (a) – retraction; (b) – extension

The results shown in Figure 7 indicate that the volumetric efficiency of the actuator decreases as the pressure inside the actuator increases. However, this decrease is negligible. The decrease in volumetric efficiency is due to the increasing deformation of the cylinder as the pressure increases and to the increase in the pressure differential on both sides of the piston.

Figures 8a and 8b present the hydraulic-mechanical efficiencies η_{hm} of an actuator with a steel cylinder. The lowest efficiencies were recorded for pressures of 2 MPa, which is due to the high proportion of frictional energy in the total energy supplied to the system. For the retraction, it is evident that an increase in the average operating pressure causes an increase in η_{hm}, while an increase in velocity causes a decrease in η_{hm}.

In Figure 8, an increase in hydraulic-mechanical efficiency is observed as the pressure inside the cylinder increases. This is explained by an improvement in the lubricating conditions in the piston (seal) – cylinder friction pair and thus a reduction in friction and resulting losses.

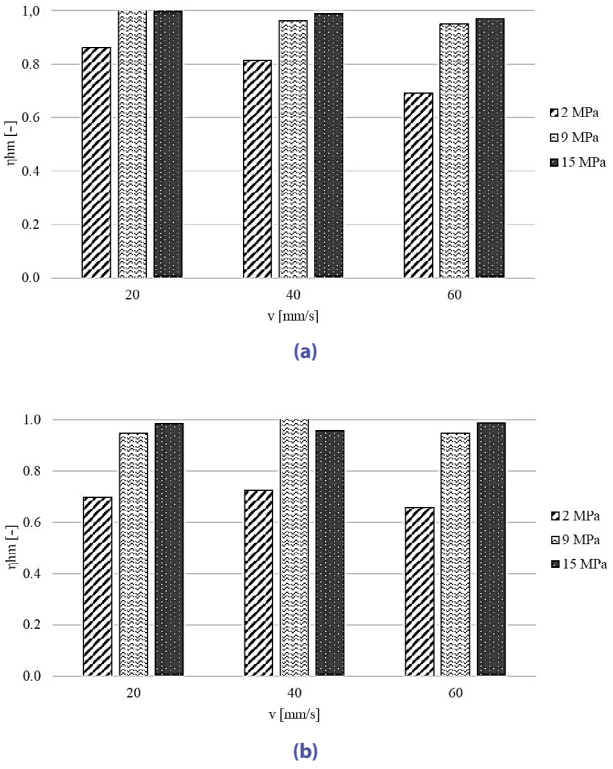

Figure 8. Hydraulic-mechanical efficiency of an actuator with a steel cylinder during: (a) – retraction; (b) – extension

4.2. The efficiency of an actuator with composite cylinder without liner

Figure 9a shows a graph of the total efficiency of a composite cylinder actuator during piston rod retraction. Efficiencies were determined for average pressures of 2 MPa, 9 MPa and 15 MPa and piston rod velocities of 20 mm/s, 40 mm/s and 60 mm/s. The lowest efficiency (35%) was recorded for a pressure of 2 MPa and a velocity of 60 mm/s, while the highest efficiency (94%) was recorded for a pressure of 15 MPa and a velocity of 20 mm/s. It can be observed that as the average pressure in the piston rod chamber increases, the total efficiency of the actuator increases, which is mainly due to a decrease in the contribution of hydraulic-mechanical losses to the energy balance. As the velocity increases, on the other hand, the total efficiency decreases slightly as a consequence of the increase in frictional forces.

The actuator behaves similarly during piston rod extension (Figure 9b). In this case, the highest efficiency (91%) was achieved at 15 MPa and 60 mm/s, while the lowest efficiency (39%) was achieved at 2 MPa and 60 mm/s.

Figure 10a and Figure 10b show the volumetric efficiencies of the actuator successively during piston rod retraction and extension. In all cases, the η_v values are between 90% and 100%.

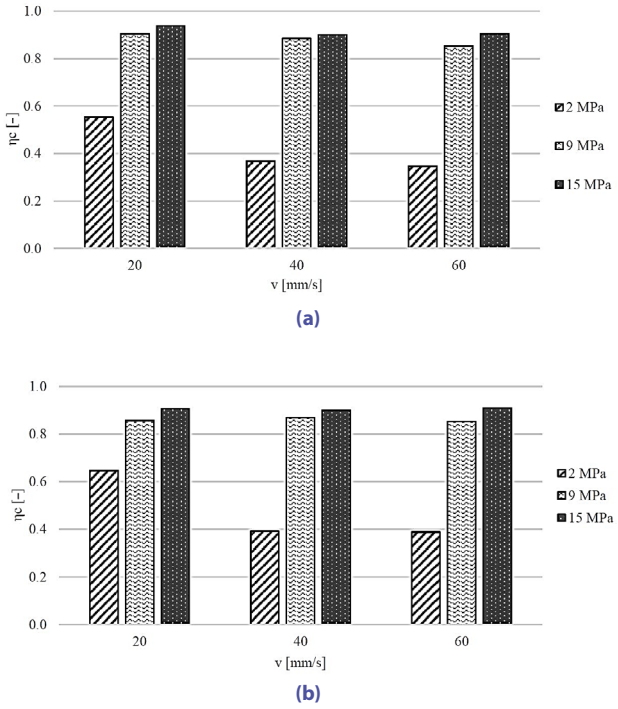

Figure 9. Overall efficiency of the composite cylinder during: (a) – retraction; (b) – extension

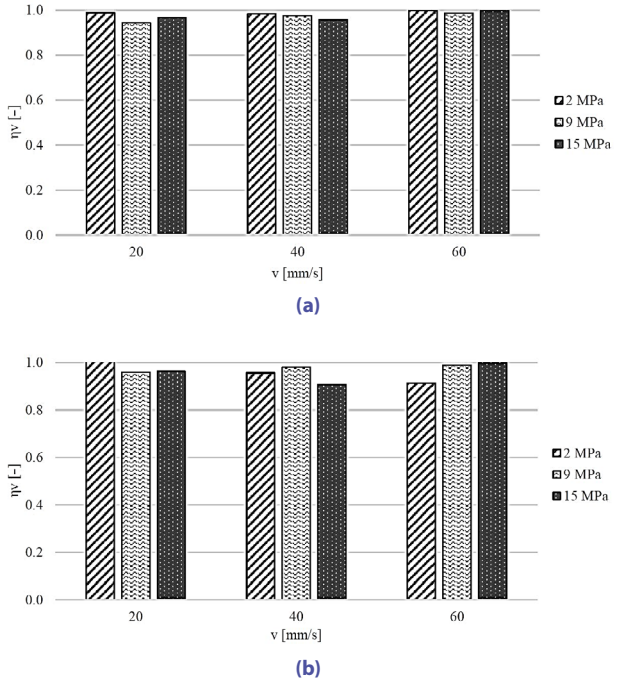

Figure 10. Volumetric efficiency of the composite cylinder during: (a) – retraction; (b) – extension

Figure 11a and Figure 11b show hydraulic-mechanical efficiency η_{hm} of a composite cylinder actuator during retraction and extension. In most cases, it can be seen that increasing the velocity leads to a decrease in η_{hm}, while increasing the load (and therefore the operating pressure) leads to an increase in η_{hm}.

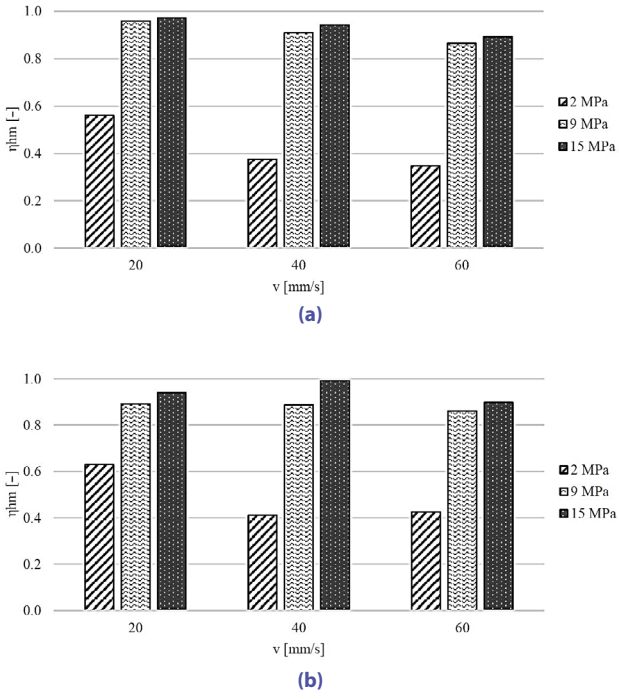

Figure 11. Hydraulic-mechanical efficiency of the actuator with composite cylinder during: (a) – retraction; (b) – extension

In Figures 11a and 11b, it can be observed that an increase in pressure inside the cylinder leads to an increase in hydraulic-mechanical efficiency, which can be explained by improved lubrication conditions in the piston (seal) – cylinder friction pair.

4.3. The efficiency of an actuator with composite cylinder without liner

Figure 12a shows a graph of the total efficiency ηc of an actuator with a composite cylinder and a polymer liner obtained during retraction. The lowest total efficiency (33%) was recorded at a pressure of 2 MPa and a velocity of 60 mm/min, while the highest (94%) was recorded at a pressure of 15 MPa and a velocity of 20 mm/min. Two trends can be observed. Firstly, total efficiency increases as the average pressure in the chamber increases. Secondly, total efficiency decreases with increasing piston velocity. Identical trends can be observed during extension (Figure 12b). In this case, the lowest (50%) and highest (92%) efficiencies were recorded for the same parameters.

Figure 13a and Figure 13b show the volumetric efficiencies η_v of the actuator at piston retraction and extension, respectively. In all cases, the values are between 90% and 100%.

Figure 14a shows the hydraulic-mechanical efficiency η_{hm} of the actuator during piston retraction. The highest value of η_{hm} (94%) was recorded at a pressure of 15 MPa and a velocity of 20 mm/min, while the lowest value (34%) was recorded at a pressure of 2 MPa and a velocity of 60 mm/min. As the pressure increases, the hydraulic-mechanical efficiency also increases in most cases, due to

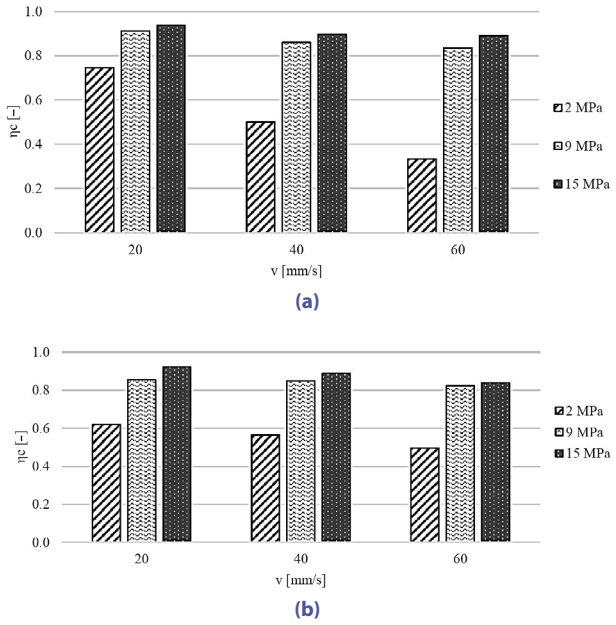

Figure 12. Overall efficiency of the actuator with composite cylinder and polymer liner during: (a) – retraction; (b) – extension

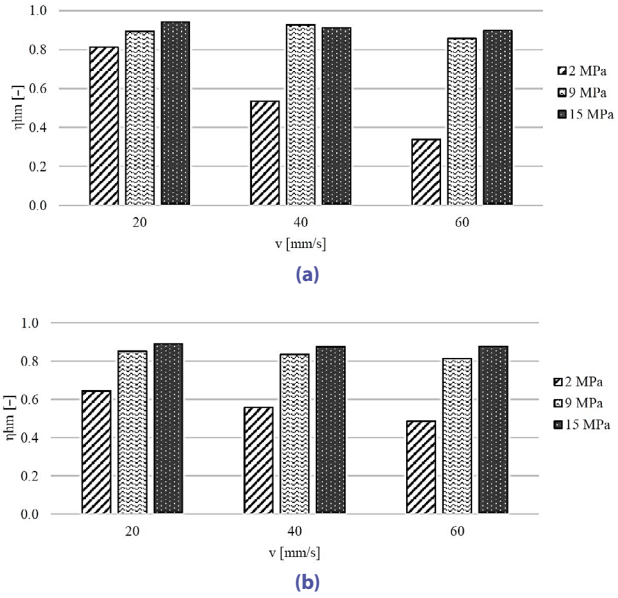

Figure 14. Hydraulic-mechanical efficiency of an actuator with composite cylinder and polymer liner during: (a) – retraction; (b) – extension

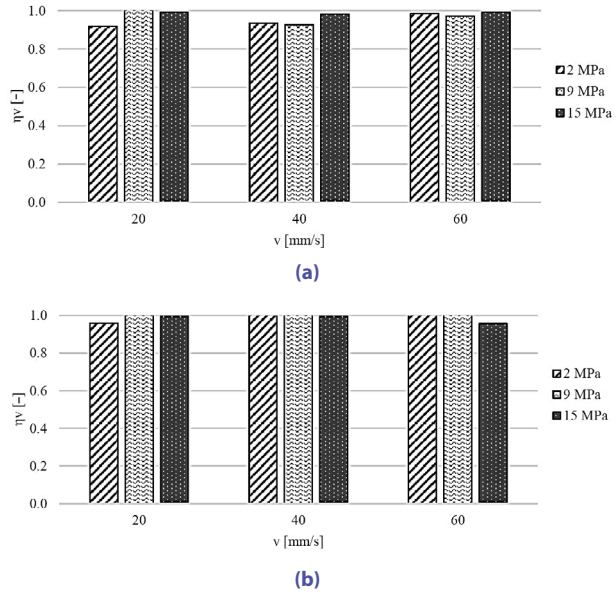

Figure 13. Volumetric efficiency of actuator with composite cylinder and polymer liner during: (a) – retraction; (b) – extension

the higher proportion of useful energy in the total energy supplied to the component (pressure does not significantly affect the amount of energy lost due to hydraulic-mechanical losses).

In addition, it can be seen in Figure 14a that an increase in stroke velocity results in a decrease in efficiency, which can be attributed to the increased frictional force between the moving parts (Popov et al., 2018). During extension (Figure 14b), very similar patterns can be observed.

Table 4 shows a comparison of the total efficiencies for the different materials used for the cylinder friction surface (steel, CFRP composite, polyurethane F180) at a nominal operating pressure of 15 MPa and the three tested piston movement velocities.

Efficiencies were averaged for the extension and retraction movements. Values for CFRP and polymer materials were related to reference values obtained for steel.

In addition, a comparison was made between the masses of the cylinders under consideration (Table 5).

As can be seen from Table 5, the greatest reduction in cylinder weight occurs for the CFRP liner. A similar weight reduction is obtained for the F180 liner. From a technological

Table 4. Comparison of average total efficiencies for different cylinder inner surface materials at 15 MPa operating pressure and three velocities

Speed	20 mm/min	difference, %	40 mm/min	difference, %	60 mm/min	difference, %
Material of the inner surface	η_c		η_c		η_c	
Steel	0.933±0.024	–	0.936±0.024	–	0.931±0.010	–
CFRP	0.922±0.029	–1.2	0.900±0.006	–3.9	0.907±0.014	–2.6
F180	0.930±0.019	–0.3	0.892±0.011	–4.7	0.865±0.035	–7.1

Table 5. Comparison of the masses of the respective cylinders

Component	Mass [g]	Difference, %
Steel cylinder	1704	–
Composite cylinder – CFRP liner	136.7	91.9
Composite cylinder – F180 liner	149.6	91.2
Composite cylinder – steel liner	552	67.6

point of view, it is easiest to use a steel liner, but the relatively smallest reduction in cylinder weight is obtained.

5. Conclusions

This paper focuses on presenting the results of hydraulic tests of the performance of a hydraulic actuator with a composite cylinder. Three different types of cylinders were considered: without liner, with steel liner and with polymer (polyurethane) liner. A steel cylinder was used as a reference. A comparison of the total efficiencies for the different materials used for the cylinder friction surface (steel, CFRP composite, polyurethane F180) at a nominal operating pressure of 15 MPa and the three tested piston movement velocities. Efficiencies were averaged for the extension and retraction movements. Values for CFRP and polymer materials were related to reference values obtained for steel. Although the highest efficiency values were obtained for the steel surface, the alternative liner materials did not deviate significantly. For the composite surface (cylinder without liner), the overall efficiencies were no more than 4% lower than the reference values. Slightly worse was the polyurethane surface, for which the greatest difference from the steel surface was –7.1%. The total efficiency values of the compared solutions are similar. It can be seen that for lower actuator piston velocities, a higher total efficiency value is observed for the F180 liner material. On the other hand, for higher velocity values (40 and 60 mm/min), higher total efficiency is observed for the CFRP material. The highest differences in total efficiency are observed for 60 mm/min.

In the case of composite surfaces, improvements in efficiency could be achieved by changing the angle of the fibres in the innermost layer, changing the reinforcement and matrix materials as well as doping the resin with particles from materials showing positive tribological properties. In the case of polymer surfaces, further research work focusing on finding more favourable materials and possibly doping them could also increase the efficiency of such a design. In both cases, it also makes sense to carry out further research focusing on the selection of the sealing material to ensure the lowest possible friction.

Disclosure statement

The Authors has no conflicts of interest to declare that are relevant to the content of this article. The Authors did not receive support from any organization for the submitted work.

References

Błażejewski, W., Barcikowski, M., Stosiak, M., Warycha, J., Stabla, P., Smolnicki, M., Bury, P., Towarnicki, K., Lubecki, M., & Paczkowska, K. (2024). A novel design of a low-pressure composite vessel with inspection opening – design, manufacturing and testing. *Alexandria Engineering Journal*, *91*, 442–456. https://doi.org/10.1016/j.aej.2024.01.078

Bogdevičius, M., Karpenko, M., & Bogdevičius, P. (2021). Determination of rheological model coefficients of pipeline composite material layers based on spectrum analysis and optimization. *Journal of Theoretical and Applied Mechanics*, *59*(2), 265–278. https://doi.org/10.15632/jtam-pl/134802

Chawla, K. K. (2012). *Composite materials. Science and engineering*. Springer. https://doi.org/10.1007/978-0-387-74365-3

Datoo, M. (1991). *Mechanics of fibrous composites*. Springer. https://doi.org/10.1007/978-94-011-3670-9

El Asswad, M., Al Fayad, S., & Khalil, K. (2018). Experimental estimation of friction and friction coefficient of a lightweight hydraulic cylinder intended for robotics applications. *International Journal of Applied Mechanics*, *10*(8), Article e1850080. https://doi.org/10.1142/S1758825118500801

Elasswad, M., Tayba, A., Abdellatif, S., & Khalil, K. (2018). Development of lightweight hydraulic cylinder for humanoid robots applications. *Proceedings of the Institution of Mechanical Engineers, Part C: Journal of Mechanical Engineering Science*, *232*(18), 3351–3364. https://doi.org/10.1177/0954406217731794

Gibson, R. F. (2016). *Principles of composite material mechanics*. CRC Press. https://doi.org/10.1201/b19626

Karpenko, M. (2022). Landing gear failures connected with high-pressure hoses and analysis of trends in aircraft technical problems. *Aviation*, *26*(3), 145–152. https://doi.org/10.3846/aviation.2022.17751

Karpenko, M., & Nugaras, J. (2022). Vibration damping characteristics of the cork-based composite material in line to frequency analysis. *Journal of Theoretical and Applied Mechanics*, *60*(4), 593–602. https://doi.org/10.15632/jtam-pl/152970

Karpenko, M., Stosiak, M., Deptuła, A., Urbanowicz, K., Nugaras, J., Królczyk, G., & Żak, K. (2023). Performance evaluation of extruded polystyrene foam for aerospace engineering applications using frequency analyses. *The International Journal of Advanced Manufacturing Technology*, *126*, 5515–5526. https://doi.org/10.1007/s00170-023-11503-0

Kaw, A. K. (2005). *Mechanics of composite materials*. CRC Press. https://doi.org/10.1201/9781420058291

Kilikevicius, A., Fursenko, A., Jurevicius, M., Kilikeviciene, K., & Bureika, G. (2019). Analysis of parameters of railway bridge vibration caused by moving rail vehicles. *Measurement and Control*, *52*(9–10), 1210–1219. https://doi.org/10.1177/0020294019836123

Liu, C., & Shi, Y. (2019). Analytical model for the winding process-induced residual stresses of the multilayered filament wound cylindrical composite parts. *Materials Research Express*, *6*(10), 1–17. https://doi.org/10.1088/2053-1591/ab3ef8

Lubecki, M., Stosiak, M., Karpenko, M., Urbanowicz, K., Deptuła, A., & Cieślicki, R. (2023). Design and FEM analysis of plastic parts of a tie-rod composite hydraulic cylinder. *Mechanika*, *29*(5), 358–362. https://doi.org/10.5755/j02.mech.31817

Lubecki, M., Stosiak, M., Skačkauskas, P., Karpenko, M., Deptuła, A., & Urbanowicz, K. (2022). Development of composite hydraulic actuators: A review. *Actuators*, *11*(12), Article 365. https://doi.org/10.3390/act11120365

Mantovani, S. (2020). Feasibility analysis of a double-acting composite cylinder in high-pressure loading conditions for fluid power applications. *Applied Sciences*, *10*(3), Article 826. https://doi.org/10.3390/app10030826

Nowak, T., & Schmidt, J. (2013). Non-linear mechanical analysis of the composite overwrapped cylinder for hydraulic applications. *Advances in Manufacturing Science and Technology*, *37*(4), 31–48. https://doi.org/10.2478/amst-2013-0030

Nowak, T., & Schmidt, J. (2014). Prediction of elasto-plastic behavior of pressurized composite reinforced metal tube by means of Acoustic Emission measurements and theoretical investigation. *Composite Structures*, *118*, 49–56. https://doi.org/10.1016/j.compstruct.2014.07.015

Nowak, T., & Schmidt, J. (2015). Theoretical, numerical and experimental analysis of thick walled fiber metal laminate tube under axisymmetric loads. *Composite Structures*, *131*, 637–644. https://doi.org/10.1016/j.compstruct.2015.06.019

Parker Hannifin Corporation. (2017). Lightraulics ® Composite Hydraulic Cylinders. *Catalogue HY07-1410/UK*. https://www.parker.com/content/dam/Parker-com/Literature/Accumulator---Cooler-Division---Europe/catalogues/cylinder/composite_cylinder/Composite-Cylinders_1410-UK.pdf

Popov, V., Voll, L., Kusche, S., Li, Q., & Rozhkova, S. (2018). Generalized master curve procedure for elastomer friction taking into account dependencies on velocity, temperature and normal force. *Tribology International*, *120*, 376–380. https://doi.org/10.1016/j.triboint.2017.12.047

Rozumek, D., & Bański, R. (2012). Crack growth rate under cyclic bending in the explosively welded steel/titanium bimetals. *Materials & Design*, *38*, 139–146. https://doi.org/10.1016/j.matdes.2012.02.014

Rozumek, D., & Macha, E. (2009). A survey of failure criteria and parameters in mixed-mode fatigue crack growth. *Materials Science*, *45*, 190–210. https://doi.org/10.1007/s11003-009-9179-2

Rozumek, D., Marciniak, Z., Lesiuk, G., & Correia, J. (2017). Mixed mode I/II/III fatigue crack growth in S355 steel. *Procedia Structural Integrity*, *5*, 896–903. https://doi.org/10.1016/j.prostr.2017.07.125

Sanchez-Sobrado, O., Visniakov, N., Bureika, G., Losada, R., & Rodriguez, E. (2024). Effect of the chemical surrounding environment on the physical and mechanical properties of aged thermoplastic polymers. *Heliyon*, *10*(2), Article e24146. https://doi.org/10.1016/j.heliyon.2024.e24146

Scholz, S., & Kroll, L. (2014). Nanocomposite glide surfaces for FRP hydraulic cylinders – evaluation and test. *Composites Part B: Engineering*, *61*, 207–213. https://doi.org/10.1016/j.compositesb.2014.01.044

Solazzi, L. (2019). Design and experimental tests on hydraulic actuator made of composite material. *Composite Structures*, *232*, Article 111544. https://doi.org/10.1016/j.compstruct.2019.111544

Solazzi, L. (2021). Stress variability in multilayer composite hydraulic cylinder. *Composite Structures*, *259*, Article 113249. https://doi.org/10.1016/j.compstruct.2020.113249

Stelling, O., Otte, B., & Petker, J. (2014). Composite high pressure hydraulic actuators for lightweight applications. In *Proceedings of the 9th International Fluid Power Conference* (*IFK*) (pp. 167–183). Semantic Scholar.

Stosiak, M., & Karpenko, M. (2024). *Synthesis lectures on mechanical engineering. Dynamics of machines and hydraulic systems*: *Mechanical vibrations and pressure pulsations*. Springer. https://doi.org/10.1007/978-3-031-55525-1

Szczepaniak, P., & Jastrzębski, G. (2020). Badania kompozytowego siłownika hydraulicznego do serwomechanizmu wspomagania sterowania śmigłowcem bezzałogowym. *Mechanica w Lotnictwie*, *ML–XIX*, 219–260. https://doi.org/10.15632/ML2020/249-260

Szydelski, Z. (1999). *Pojazdy samochodowe. Napęd i sterowanie hydrauliczne*. Wydawnictwa Komunikacji i Łączności. (in Polish).

Teijin Carbon Fiber Business. (2024). *Tenax™ Filament Yarn property*. https://www.teijincarbon.com/products/filament-yarn

Toray Composite Material America Inc. (2021). Torayca® carbon fiber selector guide. *Toray Composite Materials America*.

Ulbricht, A., Gude, M., Barfuß, D., Birke, M., Schwaar, A., & Czulak, A. (2016). Potential and application fields of lightweight hydraulic components in multi-material design. *In 10th International Fluid Power Conference* (*IFK2016*) (pp. 463–472). Technische Universität Dresden.

Vacca, A. (2021). *Hydraulic fluid power: Fundamentals*, *applications*, *and circuit design*. John Wiley and Sons Ltd. https://doi.org/10.1002/9781119569145

Wang, Z., Chen, K., & Zhan, C. (2018). Structural development and strength theory research of hydraulic cylinder CFRP Tube. *Chinese Hydraulics & Pneumatics*, *0*(07), 1–7. (in Chinese).

Wypych, G. (2016). *Handbook of polymers*. ChemTec Publishing.